scientific reports

Check for updates

OPEN

Three-dimensional characterization of caves within the Grand Canyon's deep karst aquifer

Blase LaSala[1]✉, Temuulen Tsagaan Sankey[1], Mark Nebel[2], Abraham E. Springer[3] & Aria Mildice[4]

Understanding groundwater movement within karst aquifers remains challenging because flow-defining conduit and fracture networks are both complex and inaccessible. In Grand Canyon National Park, dye tracers have been used to establish flow paths for springs that support ecosystems and park operations. Unfortunately, these point-to-point studies are limited when attempting to extrapolate flow paths over thousands of square kilometers. We introduce a mobile lidar-based methodology that resolves groundwater flow-defining structures from actively-discharging stream caves within the aquifer. This methodology enabled efficient collection of centimeter-scale 3D data from over 10 km of remote caves from the Redwall (Mississippian) and Muav (Cambrian) limestones in the North Rim of the Grand Canyon. Our methodology achieved total compounding errors of less than 0.5% and shows strong agreement with traditional cave maps. We find geologic structures exposed within these caves are consistent across kilometers of cave passages, indicating groundwater flow exploits joint sets and bedding dip direction. These patterns suggest that present-day flow paths within the North Rim of Grand Canyon National Park are, in part, a product of regional faulting and uplift. This lidar-derived structural characterization enables karst network flow pattern identification that would be otherwise unavailable from traditional methods.

Keywords Cave survey, Hydrogeology, Lidar, Remote sensing, Geoinformatics, Speleology

Karst aquifers support millions of people worldwide[2] and are critical for ecosystems and biodiversity[3,4]. However, the complexity of karst aquifers, coupled with their ability to rapidly transmit groundwater over large distances, makes them both vulnerable to contamination and challenging to model[5–8]. Traditionally, maps and surveys of solutional cave networks have been used to infer hydrogeologic properties of karst aquifers[9–11], but their accuracy and resolution can limit their utility in predicting groundwater flow[12,13]. Using Grand Canyon National Park's (GRCA) spring-based water supply as a case study, we evaluate if cave lidar can be an effective tool for characterizing regional flow paths within a remote karst aquifer at high spatial resolutions.

In the arid southwestern United States, many tribal nations, municipalities, and federal land management agencies are entirely reliant on karst aquifers for water[14,15]. Currently, Grand Canyon National Park's water supply, which supports over 6 million visitors annually, is sourced from a single cave spring within the North Rim of the canyon[16]. While the recharge area of this spring is not well defined, previous hydrologic studies on North Rim springs within the park have come to three major conclusions: (1) Discharge from North Rim springs is dominated by snowpack on the Kaibab Plateau [Fig. 1]. (2) Groundwater flow is largely conduit-based and efficient, sinking hundreds of meters and traveling up to 20 km to canyon springs in days to weeks, creating intrinsic vulnerability[17]. (3) Flow paths from sinks to springs are highly complex[18–20]. Given the proximity of these sinkholes to infrastructure and GRCA's dependence on karst-fed springs to support both ecosystems and operations, additional efforts to characterize this aquifer at higher resolutions are needed.

The rugged topography of the Grand Canyon remains an obstacle for comprehensive hydrologic study. The incision of the Colorado River exposes a multi-layered karst aquifer composed of alternating Paleozoic shales, siltstones, sandstones, and carbonates[21]. The largest springs (by discharge) for the Grand Canyon region emerge from the Redwall and Muav limestones, which lie over 700 m beneath the surface of the Kaibab Plateau[22]. No

[1]School of Informatics, Computing and Cyber Systems, Northern Arizona University, 1295 Knoles Dr, Flagstaff, AZ 86011, USA. [2]5804 E Ridge Dr, Flagstaff, AZ 86004, USA. [3]School of Earth Sciences and Environmental Sustainability, Northern Arizona University, P.O Box 4099, Flagstaff, AZ 86011, USA. [4]National Cave and Karst Research Institute, New Mexico Institute of Mining and Technology, 400-1 Cascades Ave, Carlsbad, NM 88220, USA. ✉email: bl778@nau.edu

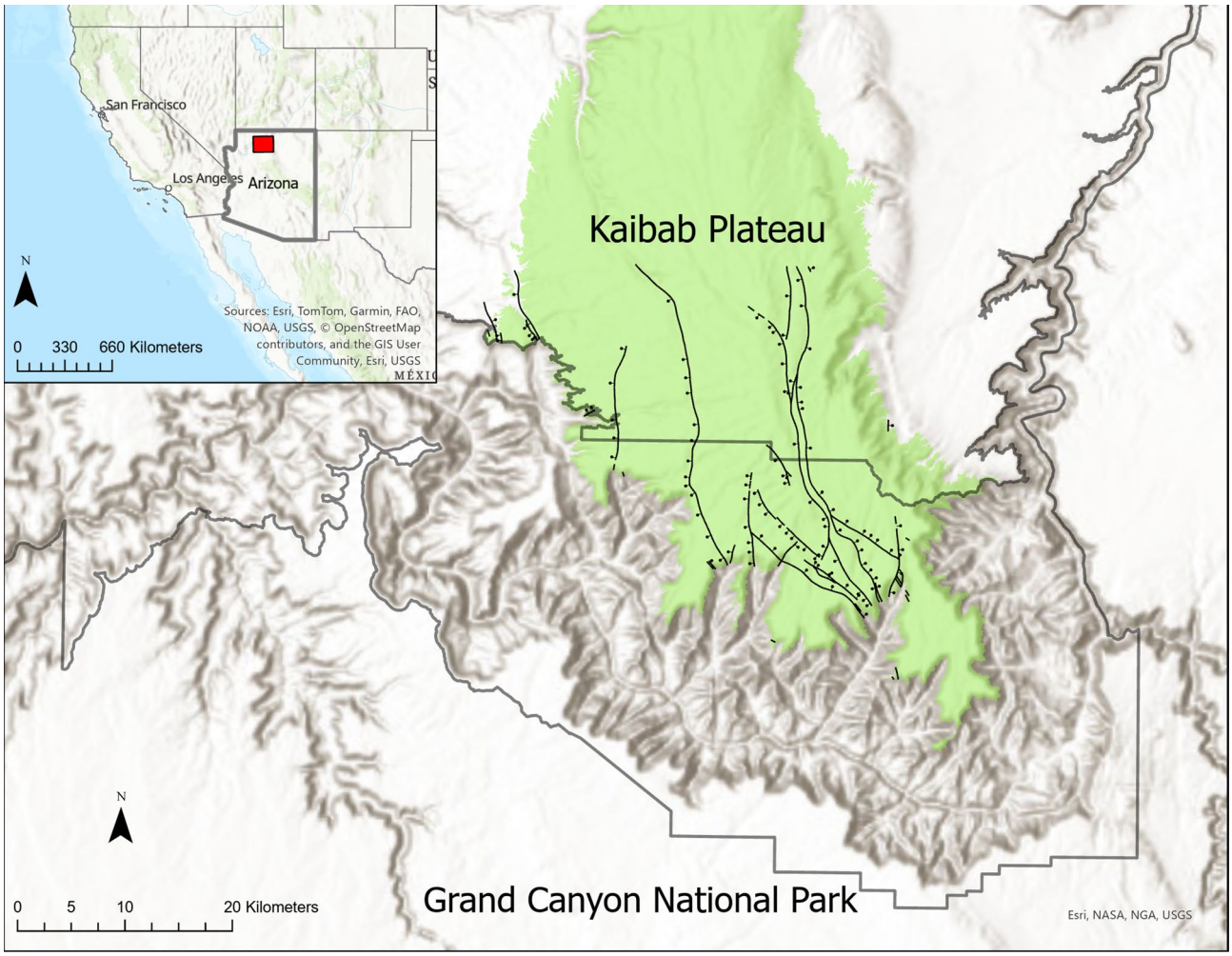

Fig. 1. An overview of the study area highlighting the Grand Canyon National Park (black outline) and the Kaibab Plateau at elevations > 2130 m (7000 ft, green shape). High-angle faulting on the plateau is shown with ball and bar symbology pointing in the direction of the downthrown block, adapted from Billingsley 2000[1] (https://pubs.usgs.gov/imap/i-2688/), USGS public domain. Maps created in Esri ArcGIS Pro 3.5.0 (https://www.esri.com).

public well logs on the plateau reach this depth, and lineament analysis and electromagnetic resistivity studies are limited in modeling general properties of this aquifer[23].

Fortunately, the exposure of these layers by the erosion of the canyon provides a rare window into the inner structures of this aquifer. Over 80 km of cave passages within the Redwall and Muav limestones have been traditionally surveyed in the past two decades[24]. Caves form in carbonate rock when groundwater maintains its chemical aggressiveness along a flow path for long distances[25]. Cave maps from these traditional surveys suggest major groundwater flow paths develop along structural weaknesses within the rock mass beneath the Kaibab Plateau's surface[26,27]. While utilizing maps to infer hydrologic properties of an aquifer is well documented[9,28,29] their two-dimensional nature and inherent subjectivity complicates analysis.

Terrestrial lidar, which measures the return time of light pulses to precisely characterize a three-dimensional space or object, has a demonstrated record of success in measuring cave environments[30–32]. In addition, extracting geologic features from lidar point clouds has been well established in the literature[33–35]. Our study objectives were to: (1) characterize caves within the Grand Canyon's North Rim with a handheld mobile laser scanner (MLS) to better understand geologic controls on groundwater flow within the rock mass directly, and (2) compare the accuracy of this methodology with other independent surveys, including cave survey and radiolocation control points.

Results

Lidar metrics

We find that mobile laser scanners (MLS) are an excellent tool for efficiently generating accurate three-dimensional models of multi-kilometer cave systems at centimeter-scale resolution. Three perennially discharging remote caves in the North Rim of the Grand Canyon were scanned, including GRCA's current water source: Roaring

Springs Cave. Over 10.2 km of passages were documented in 25 days. The average point density of these point clouds is 1,615 points/m^2 and features as small as 10 cm in diameter can be resolved. Average registration root mean squared error (RMSE) between scans was less than 10 mm, with a minimum overlap between scans of 20.1% [Table 1]. Maximum depths from cave entrances exceeded 1 km horizontally and 400 m vertically beneath the North Rim. We estimate the total compounding error of this methodology to be 0.1%, or a drift of +/− 1 m per 1 km in the X and Y dimensions using a shallower cave system as a proxy (Lava River Cave). Lidar point clouds for all cave systems were georeferenced using 3–5 control points with an average RMSE of 6.8 mm and 10.2 mm in the X and Y, respectively [Table 1]. To our knowledge, this dataset is currently the highest resolution and most extensive three-dimensional characterization of caves within the Redwall and Muav limestones.

Relationship between flow paths and geologic structures

Our lidar point cloud data show that present-day groundwater flow within the Muav and Redwall limestones exploits sub-vertical joint sets and bedding plane dip within the rock mass. From both the lidar data and traditional surveys, it is evident that collapse from solutional enlargement exposes these features as planar surfaces across all three cave systems [Fig. 2]. For both caves in the Muav limestone (Roaring Springs and Muav West), exposed bedding planes remain consistent over their overall extents, and joint sets are clearly visible between parallel passages [Fig. 3]. The lidar-documented consistency in bedding planes and parallel passages suggest flow paths in the Muav limestone preferentially enlarge joints to more closely align with the dip direction of bedding planes. While bedding and joint control is also prevalent in the Redwall East cave passages, distinct passage morphologies are also identifiable in the lidar data.

Comparison with independent surveys

We compared lidar and traditional cave survey data products. During lidar scanning efforts of the Muav West cave, an experienced survey team simultaneously mapped the cave using traditional survey methods[37–39]. While the scan team covered twice the cave distance in the same amount of time, the survey team was faster when documenting more hazardous passages, including low crawls partially filled with water. The lidar-derived cave data had 98% spatial agreement and overlap with the traditional survey-based map when superimposed in plan view [Fig. 4]. Differences between datasets occurred in isolated areas but, surprisingly, the two surveys did not diverge significantly as distance from the entrance increased. Most differences can be attributed to where the cave sketcher had to subjectively define what was a wall or a ceiling in two dimensions. However areas that were difficult to survey, such as passages that required swimming and setting survey stations on mud covered walls, also resulted in discrepancies.

We quantified the compounding errors (drift) of our scanning methodology in a more accessible and smaller cave system outside of the Grand Canyon, Lava River Cave near Flagstaff, Arizona. This proxy cave system was similar to Grand Canyon caves in length from the entrance (1 + km) and passage dimensions but was shallow enough to establish radiolocation control points from the surface to the cave. Total compounding error of the lidar derived data was measured by determining the average distance between surface control points and their subterranean counterparts in the X and Y dimensions. Pairwise point-to-point tensions were calculated using CloudCompare's Align tool[40]. Our results indicate that the error in the X and Y dimensions increased as distance from the entrance control points increased. At 500 m from the entrance the RMSE was 0.5 m of drift, increasing to 0.87 m at 1.07 km of distance from the entrance for a compounding error of ~0.1%.

Discussion

We demonstrate that mobile lidar scanners (MLS) provide an accurate and efficient method for characterizing remote cave systems in three-dimensions and enables high-resolution documentation of features directly within a karst aquifer. The methodology and equipment outlined achieved compounding errors of 0.1% over 1 km from established control points. In addition, the mobile lidar was able to scan in difficult areas, including partially flooded crawls, climbs, and rappels. Contiguous models of multi-kilometer cave systems enable relationships between passages to be quantified, which we use to better understand how geologic structures influence modern-day aquifer flow paths. While traditional cave survey equipment is currently lighter and more durable, MLS provides more objective and higher resolution data for geologic characterization compared to traditional cave maps.

We find MLS point clouds are valuable for quantifying orientations of geologic structures that control aquifer flow paths, particularly when highlighting relationships between structures across cave passages. Traditional cave maps, especially their two-dimensional nature and focus as a navigational tool limit their utility in characterizing ceilings and walls, where important geologic structures are exposed. In addition, hand-sketched maps are more subjective and rely on the experience of the cartographers to determine what features to prioritize on the map. In this study, we document handheld lidar scanners to be faster than sketch-based traditional surveys for data

Location (AZ)	Cave	Scans Registered	Avg Error (mm)	MaxError (mm)	MinOverlap (%)
GRCA	Roaring Springs	32	5.7	6.8	20.1
GRCA	Muav West	25	7.3	8.9	36
GRCA	Redwall East	27	6.8	11.2	22
Flagstaff	Lava River Cave	9	5.7	6.5	13.7

Table 1. Lidar point cloud scan registration metrics for each cave system.

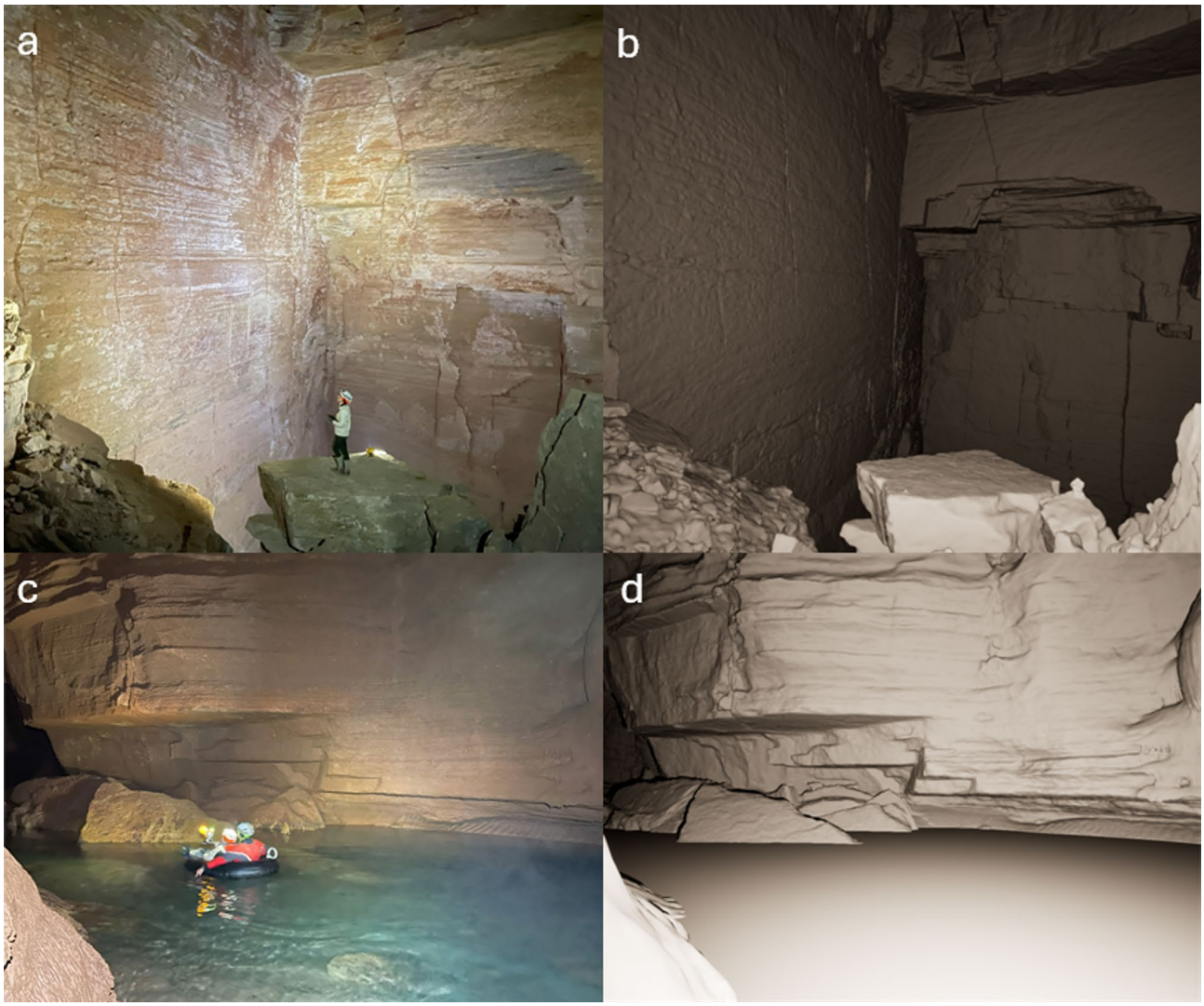

Fig. 2. A comparison of in-cave photos (left panels a, c) and a lidar-derived model (right panels b, d) of Muav Cave West showcasing planar features exposed by collapse. Joints (top panels a, b) and bedding planes (bottom panels c, d) orientations control groundwater flow direction. The cave model consists of 750 million polygons, with an average edge length of 2 cm. This model was generated using Poisson Reconstruction[36]. Water surface on the bottom left panel is manually added as a featureless plane.

acquisition, but suboptimal on climbs and partially flooded passages with less than 30 cm of airspace. While this study is focused on bedding planes, joints and passage morphologies, features with dimensions > 10 cm are visible.

Lidar data application: Understanding aquifer flow paths

Given these encouraging results, we compare our lidar-derived findings to previous predictions and past studies on groundwater flow within the Kaibab plateau. Lidar data from all three GRCA caves show flow paths within the Redwall and Muav limestones developing along subvertical joint sets along bedding plane dip [Fig. 3]. This control on passage morphology is consistently observed in the lidar data, despite the three caves being located on opposite sides of the North Rim over 30 km apart. This pattern supports the longstanding hypothesis that groundwater flow, karst and cave development in the Redwall-Muav carbonates are concentrated along sub-parallel joint sets related to regional faults[26,27]. Given the increased densities of sinkholes near normal fault complexes[17], our results indicate modern day flow paths within the Kaibab Plateau are, at least in part, a product of a tectonic extensional regime.

One notable difference between the Redwall and the Muav cave passage morphologies was the evidence of phreatic (below water table) cave development in the Redwall East cave. Hypogene speleogenesis can occur when upwelling "deep" groundwater mixes with epigenetic (surface) water[41,42] and is characterized by the presence of distinct formations. Hypogene formations, such as bubble trails, blind cupolas, and three-dimensional maze passages were present in sections above the stream passage of the Redwall East lidar-derived model [Fig. 5]. These features are consistent with stable isotope results from nearby springs, which suggest that deeper upwelling

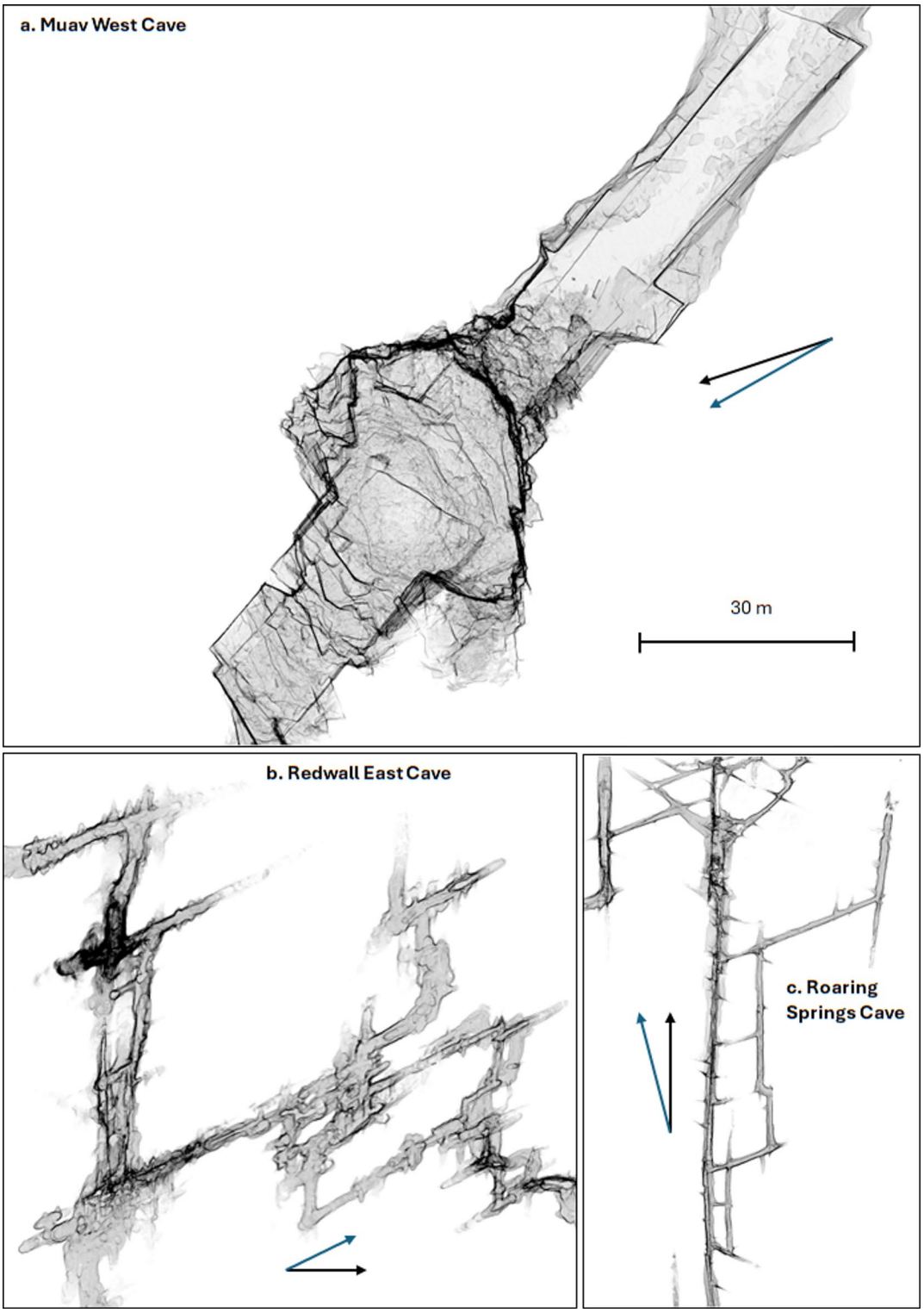

Fig. 3. Top-down view of cave lidar data highlighting straight walls (a) and parallel passages (b, c) created by solutional enlargement of sub-vertical joint sets. Arrows correspond to approximate cave stream flow direction (blue) and bedding dip direction (black) averaged over each cave. The consistency of these features across kilometers of passages suggests development of flow paths forms along joint sets within both the Redwall and Muav limestones. Scale bar applies to all caves. 3 cartography created by A. Mildice

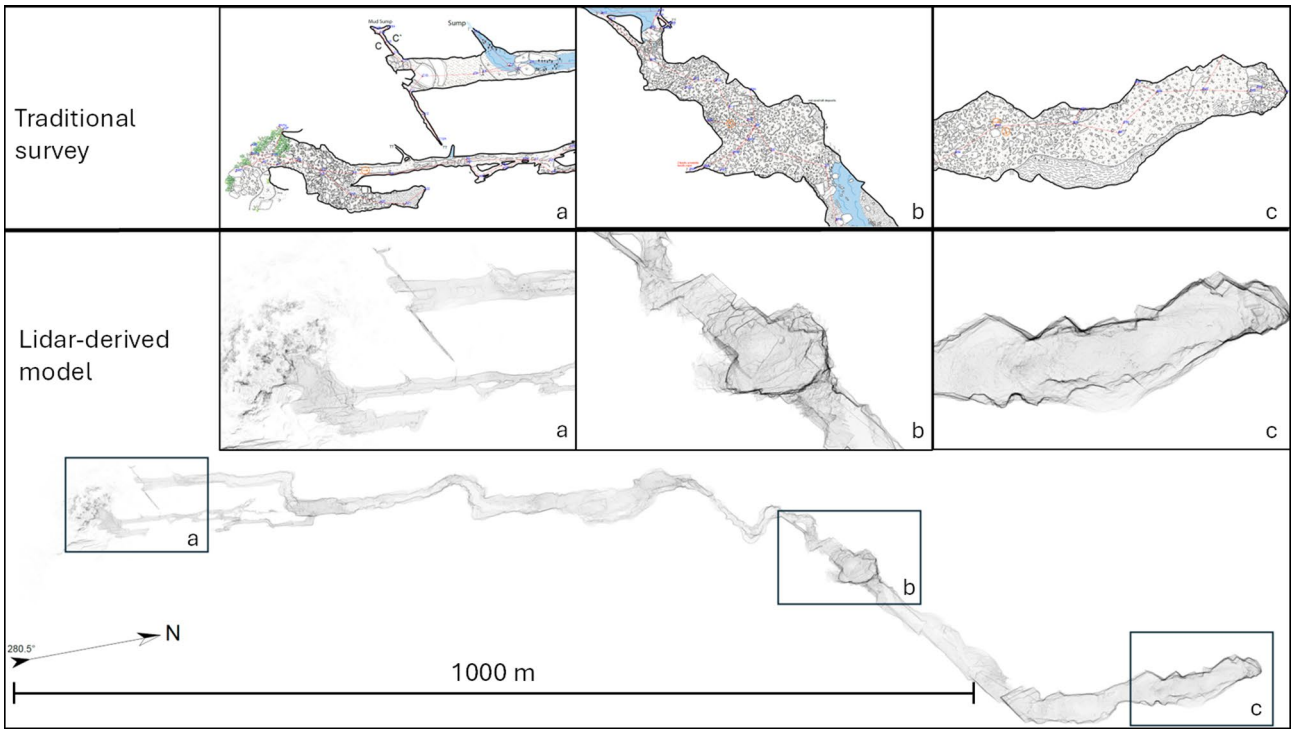

Fig. 4. A top-down view comparing traditional cave survey with lidar-derived model of the Muav West Cave. While both surveys were done independently, the two datasets are remarkably consistent over the extent of the cave. Additional panels of zoomed-in views of the entrance (a), midpoint (b), and end (c) of the cave provided to show greater details. Cartography by A. Mildice.

groundwater is a partial contributor to snowmelt-dominated discharge[20,43–45]. Given the age of speleothems within other Redwall caves on the North Rim of the Grand Canyon[46] the presence of these structures above the stream channel suggests present-day groundwater flow may utilize paleo-aquifer flow paths.

Conclusion

This study demonstrates that mobile lidar scanners are viable tools for efficiently documenting hazardous GPS-denied environments. We digitized over 10 km of remote cave passages beneath the North Rim of the Grand Canyon at previously unattainable resolutions. Our methodology enabled successful scanning through cave passages partially filled with water, crawlways less than 0.5 m in diameter, and on vertical cliffs using technical rope expertise. While adoption of lidar for cave documentation is not widespread, our results show mobile lidar data provides a detailed contiguous three-dimensional representation of caves that are less subjective than traditional surveys. This method allows for accurate identification and extraction of structural features and bedding planes that are related to groundwater flow and cave development. We achieved compounding errors of 0.1%, or a drift of 1 m per 1 km of cave passage, when comparing our methodology to control data. Validating previous predictions, we find cave development within the Redwall and Muav limestones utilize subvertical joint sets and bedding dip direction in three caves across the eastern, southern, and western flanks of the North Rim. This detailed characterization of the Redwall and Muav limestones shows consistent flow path trends, presenting mechanisms governing Kaibab plateau groundwater-flow systems.

Methods

Three caves connected to perennial springs were selected for scanning. Connectivity between sinks of the Kaibab Plateau and selected caves was established through previous tracer studies and discharge measurements from the Grand Canyon National Park Science and Resource Management Division[17,23].

In-cave scanning methods

Methodology and equipment for data collection and processing was identical for all caves. A simultaneous localization and mapping (SLAM) near-infrared (905 nm) handheld mobile lidar scanner (MLS) (GeoSLAM Zeb Horizon, Ltd. Nottingham, UK) was used to generate three-dimensional point clouds of all passages. The GeoSLAM scanner has 6 mm relative accuracy, as reported by the vendor, and records 300,000 points a second at ranges up to 100 m. All scans were completed as a loop, with the scanner starting and stopping at the same exact position to minimize error and data gaps using a tripod mounted frame. Scan duration was limited to < 25 min and laser returns over 30 m from the scanner were discarded to maintain precision[47]. To mitigate the chance of data corruption, scans requiring the scanner to be transported through low airspaces, or up and down cliffs were

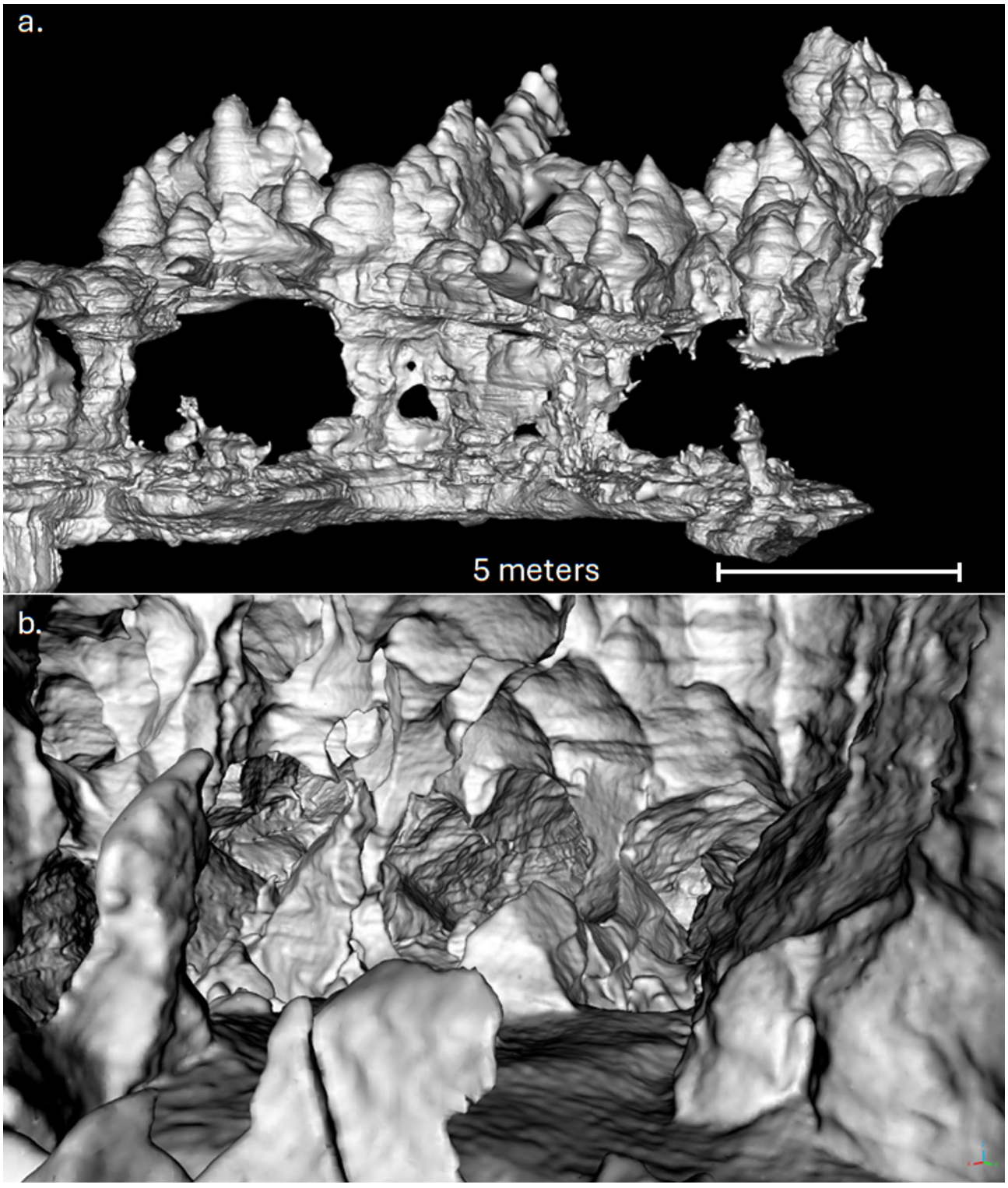

Fig. 5. Three-dimensional renders of a section of Redwall East Cave point cloud enable visualization of passage morphologies that are traditionally difficult to portray in two dimensions. Viewed in profile (a), distinctive conical ceiling features and vertical connectivity between passages are apparent. Looking from within the model (b) the geometrically complex network of passages is accurately modelled.

done twice for redundancy. Scans in crawls less than 0.5 m in diameter were completed with the scanner pointed towards previously scanned passage to allow the SLAM algorithm to match features more easily. Transporting the scanner across hazardous areas, such as deep water and climbs, was accomplished by handing off the scanner to a securely positioned assistant. Consequently, extraneous points in the lidar point cloud were removed manually. A minimum overlap of 10 m between scans was maintained to facilitate registrations between adjacent scans.

Georeferencing and data processing

All cave point clouds in this study were georeferenced using 3–5 control points recorded from each cave's entrance scan. If no established control points were available in near the entrance, a Leica GG04 + GNSS antenna with Precise Point Positioning was used to record latitude, longitude (WGS84) and elevation above the geoid (EGM 2008). Geodetic coordinates were projected into grid and then ground coordinate reference systems (CRS) using a combined scale factor (CSF) from a central point with the lowest RMSE. CSF was calculated using the National Oceanic and Atmospheric Administration's (NOAA) and National Geodetic Survey's (NGS) "NCAT" and "vDatum" tool[48].

For the proxy cave system (Lava River Cave), additional at-depth control points were recorded at the midpoint and end of the proxy cave using longwave radiolocation antennae. A 25 cm diameter radio transmitter was levelled over each control point in the cave, emitting a quasi-static magnetic field at 3946 Hz[49]. A 42 cm radio antenna was used to locate the null, or center of this field on the surface, where a GPS coordinate was recorded.

Lidar scans were exported from the lidar unit with FARO Connect (ver. 2024.4.0) using the "standard" preset with the "transient" filter enabled with no subsampling. Critically, scans were exported using a filetype that enabled "normals" to be saved for each point to facilitate converting the clouds to meshes. A continuous end-to-end model for each cave was generated by manually registering scans together using FARO SCENE (ver. 2018.0.0648). Registration error between scans was determined using FARO SCENE's cloud-to-cloud registration at default settings for each cave system. The resulting cave clouds were spatially subsampled to a minimum distance of 1 mm between points.

Traditional cave survey methods

A traditional cave survey was conducted during scanning efforts for Muav West Cave in October 2022, with an additional trip in October 2023. Data collection methods were based on established cave survey techniques[37–39]. The survey team used three modified Leica e7400x distometers ("Disto X2's") to measure distance, inclination, and azimuth between stations. Instrument calibration was conducted in the field before survey, attaining an average error of $< 0.4°$ for each DistoX2 with a standard deviation of $< 0.3°$. Cross checking of measurements by independently backsighting each survey shot ensured azimuth and inclination measurements were within 2° of agreement. Survey shot distance measurements were only recorded if their independently measured backsight agreement was < 6.1 cm (0.2 ft). A 2D sketch of the cave was drawn around these measurements in plan view, with cross sections at each survey station. Measurements from surveys were digitized using COMPASS Cave Survey Software[50]. Sketches of the cave were combined to create a seamless map using Adobe Illustrator. Inventory of formations, sediments, biology, and human impacts was done for all survey stations[51].

Data availability

The data that support the findings of this study are available from Grand Canyon National Park, but restrictions apply to the availability of these data, which fall under the Federal Cave Resources Protection Act of 1988, and so are not publicly available. Data are however available from the corresponding author upon reasonable request and with permission of Grand Canyon National Park.

Received: 1 April 2025; Accepted: 25 August 2025
Published online: 30 August 2025

References

1. Billingsley, G. H. Geologic map of the Grand Canyon 30'x 60'quadrangle, Coconino and Mohave Counties, northwestern Arizona US Geological Survey Report (No. 2688). (2000).
2. Stevanović, Z. Karst waters in potable water supply: A global scale overview. *Environ. Earth Sci.* **78** (23), 662 (2019).
3. Clements, R., Sodhi, N. S., Schilthuizen, M. & Ng, P. K. Limestone karsts of Southeast asia: imperiled arks of biodiversity. *Bioscience* **56** (9), 733–742 (2006).
4. Gunn, J. Karst groundwater in UNESCO protected areas: a global overview. *Hydrogeol. J.* **29** (1), 297–314 (2021).
5. Medici, G., Munn, J. D. & Parker, B. L. Delineating aquitard characteristics within a silurian dolostone aquifer using high-density hydraulic head and fracture datasets. *Hydrogeol. J.* **32** (6), 1663–1691 (2024).
6. Parise, M., et al. Hazards in karst and managing water resources quality. *Karst aquifers—Characterization and engineering*. 601–687 Cham: Springer International Publishing. (2015).
7. Hartmann, A., Goldscheider, N., Wagener, T., Lange, J. & Weiler, M. Karst water resources in a changing world: review of hydrological modeling approaches. *Rev. Geophys.* **52** (3), 218–242 (2014).
8. Vesper, D. J., Loop, C. M. & White, W. B. Contaminant transport in karst aquifers. *Theoretical Appl. Karstology*. **13** (14), 101–111 (2001).
9. Palmer, A. N. Origin and morphology of limestone caves. *Geol. Soc. Am. Bull.* **103** (1), 1–21 (1991).
10. Groves, C. & Meiman, J. Weathering, geomorphic work, and karst landscape evolution in the Cave City groundwater basin, Mammoth Cave, Kentucky. *Geomorphology* **67** (1–2), 115–126 (2005).
11. Šebela, S. Structural geology of the Škocjan Caves. *Acta carsologica,* **38** (2–3), (2009).
12. Ballesteros, D., Jiménez-Sánchez, M., García-Sansegundo, J. & Giralt, S. Geological methods applied to speleogenetical research in vertical caves: the example of Torca Teyera shaft (Picos de europa, Northern Spain). *Carbonates Evaporites.* **26**, 29–40 (2011).
13. Jouves, J. et al. Speleogenesis, geometry, and topology of caves: A quantitative study of 3D karst conduits. *Geomorphology* **298**, 86–106 (2017).

14. Tobin, B. W., Springer, A. E., Kreamer, D. K. & Schenk, E. The distribution, flow, and quality of Grand Canyon Springs, Arizona (USA). *Hydrogeology Journal,* **26**(3), (2018).
15. Bills, D. J. & Flynn E., M. Hydrogeologic data for the Coconino plateau and adjacent areas, Coconino and Yavapai counties, Arizona (2002 – 265). *US Geol. Surv.* https://doi.org/10.3133/ofr02265 (2007).
16. National Park Service, Grand Canyon. Transcanyon Waterline Project. https://www.nps.gov/GRCA/getinvolved/tcwl.htm, Accessed 10/1/2022. (2022).
17. Jones, N. A., Hansen, J., Springer, A. E., Valle, C. & Tobin, B. W. Modeling intrinsic vulnerability of complex karst aquifers: modifying the COP method to account for sinkhole density and fault location. *Hydrogeol. J.* **27** (8), 2857–2868 (2019).
18. Chambless, H. E., Springer, A. E., Evans, M. & Jones, N. Deep-karst aquifer spring-flow trends in a water-limited system, grand Canyon National park, USA. *Hydrogeol. J.* **31** (7), 1755–1771 (2023).
19. Jones, C. J., Springer, A. E., Tobin, B. W., Zappitello, S. J. & Jones, N. A. Characterization and hydraulic behaviour of the complex karst of the Kaibab plateau and grand Canyon National park, USA. *Geol. Soc. Lond. Special Publications*. **466** (1), 237–260 (2018).
20. Crossey, L. J. et al. Hydrotectonics of Grand Canyon Groundwater. *Annual Rev. Earth Planet. Sciences* **52**, (2024).
21. Beus, S. S. & Billingsley, G. H. Paleozoic strata of the Grand Canyon, Arizona. *Geology of Grand Canyon, Northern Arizona (with Colorado River Guides): Lee Ferry to Pierce Ferry, Arizona*, **115**, 122–127. (1989).
22. Knight, J. E. & Huntoon, P. W. Conceptual models of groundwater flow in the Grand Canyon region, Arizona: U.S. *Geological Survey Scientific Investigation Report 2022–5037*, 51, https://doi.org/10.3133/sir20225037. (2022).
23. Gettings, M. E. & Bultman, M. W. Candidate-penetrative-fracture mapping of the grand Canyon area, arizona, from Spatial correlation of deep geophysical features and surficial lineaments. *USGS Report*, 9. (2005).
24. Tobin, B. W., Springer, A. E., Ballensky, J. & Armstrong, A. Cave and karst of the grand Canyon world heritage site. *Z. Fur Geomorphologie Supplement*. **62** (3), 125–144 (2021).
25. Palmer, A. N. Patterns of dissolution porosity in carbonate rocks. *Karst Model. Karst Water Inst. Sp Publ*. **5**, 71–78 (1999).
26. Huntoon, P. W. The karstic groundwater basins of the Kaibab plateau, Arizona. *Water Resour. Res.* **10** (3), 579–590 (1974).
27. Huntoon, P. W. Variability of karstic permeability between unconfined and confined aquifers, grand Canyon region, Arizona. *Environ. Eng. Geoscience*. **6** (2), 155–170 (2000).
28. Palmer, A. N. Cave exploration as a guide to geologic research in the Appalachians. *J. Cave Karst Stud.* **71** (3), 180–192 (2009).
29. Horrocks, R. D. & Szukalski, B. W. Using geographic information systems to develop a cave potential map for wind cave, South Dakota. *J. Cave Karst Stud.* **64**(1), 63–70 (2002).
30. Šupinský, J., Kaňuk, J., Nováková, M. & Hochmuth, Z. LiDAR point clouds processing for large-scale cave mapping: A case study of the Majko dome in the domica cave. *J. Maps*. **18** (2), 268–275 (2022).
31. Shazali, N. et al. Assessing Bat roosts using the lidar system at wind cave nature reserve in sarawak, Malaysian Borneo. *Acta Chiropterologica*. **19** (1), 199–210 (2017).
32. Idrees, M. O. & Pradhan, B. A decade of modern cave surveying with terrestrial laser scanning: A review of sensors, method and application development. *International J. Speleology* **45**(1), (2016).
33. Zhang, J. & Singh, S. Low-drift and real-time lidar odometry and mapping. *Auton. Robots*. **41**, 401–416 (2017).
34. Daghigh, H., Tannant, D. D., Daghigh, V., Lichti, D. D. & Lindenbergh, R. A critical review of discontinuity plane extraction from 3D point cloud data of rock mass surfaces. *Comput. Geosci.* **169**, 105241 (2022).
35. Gigli, G. & Casagli, N. Semi-automatic extraction of rock mass structural data from high resolution LIDAR point clouds. *Int. J. Rock Mech. Min. Sci.* **48** (2), 187–198 (2011).
36. Kazhdan, M. & Hoppe, H. Screened Poisson surface reconstruction. *ACM Trans. Graphics (ToG).* **32** (3), 1–13 (2013).
37. Dasher, G. R. *On Station: A Complete Handbook for Surveying and Mapping Caves.* Second Edition National Speleological Society, (2011).
38. Bristol, D. *Cave survey*. https://www.derekbristol.com/survey-overview, Accessed 7/4/2025 (2023).
39. Harley, G. L., Polk, J. S., North, L. A. & Reeder, P. P. Application of a cave inventory system to stimulate development of management strategies: the case of west-central Florida. USA. *J. Environ. Management* **92** (10), 2547–2557 (2011).
40. Girardeau-Montaut, D. & CloudCompare. *France: EDF R&D Telecom ParisTech*, **11**(5), 2016 (2016).
41. Palmer, A. N. Distinction between epigenic and hypogenic maze caves. *Geomorphology* **134** (1–2), 9–22 (2011).
42. Klimchouk, A. B. Hypogene speleogenesis: Hydrogeological and Morphogenetic Perspective. *NCKRI-Special Paper 1* (2007).
43. Crossey, L. J. et al. Degassing of mantle-derived CO2 and he from springs in the Southern Colorado plateau region—Neotectonic connections and implications for groundwater systems. *Geol. Soc. Am. Bull.* **121** (7–8), 1034–1053 (2009).
44. McGibbon, C., Crossey, L. J. & Karlstrom, K. E. Fence springs of the grand canyon, USA: insight into the karst aquifer system of the Colorado plateau region. *Hydrogeol. J.* **30** (8), 2379–2398 (2022).
45. Hill, C. A. & Polyak, V. J. Karst hydrology of grand canyon, arizona, USA. *J. Hydrol.* **390** (3–4), 169–181 (2010).
46. Polyak, V., Hill, C. & Asmerom, Y. Age and evolution of the grand Canyon revealed by U-Pb dating of water table-type speleothems. *Science* **319** (5868), 1377–1380 (2008).
47. Kidd, J. R. Performance evaluation of the Velodyne VLP-16 system for surface feature surveying (*Master's thesis, University of New Hampshire*). (2017).
48. Myers, E. et al. VDatum and strategies for national coverage. In *OCEANS* 1–8 *IEEE*. (2007).
49. Raab, F. H. Quasi-static magnetic-field technique for determining position and orientation. *IEEE Trans. Geosci. Remote Sens.* **4**, 235–243 (1981).
50. Fish, L. Computer modeling of cave passages. *Compass Tape*. **15** (1), 19–24 (2001).
51. Kovarik, J. & Kambesis, P. Cave resource inventories: Why are they important. In *Proceedings of the 2005 National Cave and Karst Management Symposia*, Albany, NY, USA **270**. 745–5201 (2005).

Acknowledgements

Special thanks to Grand Canyon National Park for supporting this research. Study #: GRCA-00003 Co-op Agreement: TA P21AC10806. Research permits: GRCA-2021-SCI-0009 GRCA-2022-SCI-0003 GRCA-2023-SCI-0007. Contributors: Andy Armstrong, Zev Axler, Jason Ballensky, Jesse Bardem, Dave Bunnell, Hannah Chambless, Michael Day, Erin Dundas, Max Evans, Hailey Galit, Alicyn Gitlin, Paul Jorgenson, Ray Keeler, Garrison Loope, Abigail Mack, Dillon Metcalfe, Belinda Norby, Clint Poole, Jessica Pruitt, Danielle Urich, Bev Shade, Benjamin Tobin, Mike Van Note. Grants: Scanner purchase funding was provided in-part by the Water Resources Research Center: Water Resources Research Act, Sect. 104(b) is funded through the U.S. Geological Survey.

Author contributions

B.L, T.S, M.N, AE.S and A.M wrote the main manuscript text. B.L and A.M collected and processed the data. B.L created Figs. 1, 2, 4 and 5. B.L and A.M co-created figure 3. All authors reviewed the manuscript.

Declarations

Competing interests
The authors declare no competing interests.

Additional information
Correspondence and requests for materials should be addressed to B.L.

Reprints and permissions information is available at www.nature.com/reprints.

Publisher's note Springer Nature remains neutral with regard to jurisdictional claims in published maps and institutional affiliations.